Supporting Information

Surfactant-assisted morphology modification of nanostructured $MnMoO_4$ for high-performance asymmetric supercapacitors

Kumcham Prasad[1], TVM Sreekanth[2], Kisoo Yoo[2,*], Jonghoon Kim[1,*]

[1]*Energy storage and conversion laboratory, Department of Electrical Engineering, Chungnam National University, Daejeon, 34134, South Korea.*

[2]*School of Mechanical Engineering, Yeungnam University, Gyeongsan-si, 38541, South Korea*

Corresponding author: kisooyoo@yu.ac.kr (Prof. Kisoo Yoo)

whdgns0422@cnu.ac.kr (Prof. Jonghoon Kim)

Experimental section

Physical characterization

The phase formation and crystallinity of the MMO samples were analyzed using a PANalytical X'Pert Pro X-ray diffractometer with Cu Kα radiation source ($\lambda = 1.540$ Å) operating at 40 kV and 30 mA. The chemical bonds present in the samples were examined using a Fourier transform infrared spectrometer (FT-IR, Perkin Elmer, USA). An UV Raman spectrometer (Horiba Jobin Yvon HR 800) was used to record Raman spectra of the samples in the backscattering mode of 200 – 1000 cm^{-1} with an Nd: YAG laser source (= 532 nm). The surface morphology of the samples was examined using a S-4800, Hitachi, Japan, scanning electron microscope and EDX analysis was carried out with an X-ray column attached to the FESEM instrument. The high-resolution transmission electron microscopy images of the samples were recorded using a HRTEM, Tecnai G^2 F20 S-Twin, USA with a field-emission electron gun operated at 200 kV in Schottky mode. The chemical composition and oxidation states of the samples were quantifies with an X-ray photoelectron spectrometer (XPS, K-alpha, Thermo Scientific, USA) utilizing a monochromatic Al Kα X-ray source (1486.6 eV). A 3-Flex, Micromeritics, USA, surface analyser was used to study the surface characteristics of the samples.

Electrochemical measurements

All the electrochemical experiments were carried out at room temperature on a Biologic VSP-150 electrochemical workstation. A three-electrode system was used for the measurements in 6.0 M KOH aqueous electrolyte utilizing the as-prepared MMO electrodes as working electrodes, platinum mesh as counter electrode and Hg/HgO as reference electrode. The electrochemical techniques such as cyclic voltammetry (CV), galvanostatic charge-discharge (GCD) and electrochemical impedance spectroscopy (EIS) were used to evaluate the electrochemical performance of the electrodes. The practical application of the electrodes is tested by fabricating an asymmetric (ASC) supercapacitor device using MMO-C as a cathode, activated carbon (AC) as an anode and Whatman filter paper as a separator. A solid-state electrolyte was prepared by dissolving 3g of PVA and 3g of KOH in 20 mL of water separately. Then the KOH solution was added drop-wise to the PVA solution under continuous magnetic stirring at 85 °C for 4h. The PVA-KOH was obtained after 12h at room temperature. Then the MMO-C, AC electrodes and separator were dipped in the electrolyte for 10 minutes and dried for 12h at room temperature to evaporate the excess water. The electrodes were then assembled face-to-face using the filter paper as an ion-porous separator between them. The ASC device was tested as long as the electrolyte was solidified. The following equations were used to determine the specific capacitance, energy and power densities of the device.

$$C_s = \frac{I \times \Delta t}{M \times \Delta V} \quad \text{(S1)}$$

$$E = \frac{I \int V\, dt}{M \times 3.6} \quad \text{(S2)}$$

$$P = \frac{3600 \times E}{\Delta t} \quad \text{(S3)}$$

where, I stands for applied current in Amperes, Δt stands for discharging time in seconds, M stands for total active mass loaded on both the electrodes in grams, ΔV for potential window and ∫ V(t) dt is the integrated area of discharge curves.

Table S1: The peak positions and d-spacing values of MMO samples in comparison with standard data obtained from XRD spectra.

hkl	2θ (°)				d-spacing (Å)			
	Standard value	Observed value			Standard value	Observed value		
		MMO	MMO-P	MMO-C		MMO	MMO-P	MMO-C
(-201)	18.276	18.923	18.771	18.834	4.735	4.686	4.724	4.708
(021)	22.730	22.762	22.693	22.821	3.909	3.904	3.915	3.894
(201)	24.709	24.746	24.654	24.751	3.600	3.595	3.608	3.594
(220)	25.766	25.803	25.767	25.819	3.455	3.450	3.455	3.448
(002)	25.969	26.774	26.721	26.719	3.428	3.327	3.334	3.334
(-311)	27.766	27.834	27.781	27.846	3.210	3.203	3.209	3.201
(112)	31.256	31.279	31.279	31.345	2.859	2.857	2.857	2.851
(-222)	33.046	33.134	33.081	33.129	2.708	2.702	2.706	2.702
(400)	35.710	35.731	35.625	35.713	2.512	2.511	2.518	2.512
(-132)	37.941	37.851	37.798	37.897	2.370	2.375	2.378	2.372
(-113)	39.078	39.123	39.070	39.153	2.303	2.301	2.304	2.299
(222)	40.449	40.395	40.395	40.409	2.228	2.231	2.231	2.230
(-332)	42.840	42.674	42.780	42.781	2.109	2.117	2.112	2.112
(113)	44.029	44.052	44.105	44.108	2.055	2.054	2.052	2.052
(421)	45.918	45.695	45.695	45.693	1.975	1.984	1.984	1.984
(332)	51.875	52.055	51.896	51.974	1.761	1.755	1.760	1.758
(422)	54.455	54.440	54.387	54.486	1.684	1.684	1.686	1.683
(024)	57.064	57.143	57.143	57.128	1.613	1.610	1.611	1.608
(620)	58.363	58.415	58.256	58.384	1.580	1.579	1.582	1.579
(-533)	59.666	59.528	59.475	59.641	1.548	1.552	1.553	1.549
(-153)	62.470	62.390	62.600	62.412	1.485	1.487	1.483	1.487

Table S2: Unit cell parameters of MMO samples.

Sample	Lattice parameters	Cell volume	Crystallite size

	a (Å)	**b (Å)**	**c (Å)**	β (°)		
MMO	10.463	9.500	7.135	106.382	680.42	19.83
MMO-P	10.433	9.527	7.117	105.829	680.57	20.95
MMO-C	10.493	9.463	7.126	106.304	679.12	18.19

72

Table S3: The specific capacitance of the present work in comparison with different $MnMoO_4$-based materials.

Electrode Material	Synthesis method	Electrolyte	Specific capacitance	Cycle stability	Ref.
α-$MnMoO_4$/graphene composite	Hydrothermal	1.0 M Na_2SO_4	364 F g^{-1} @ 2 A g^{-1}	88%, 1000 cycles @ 8 A g^{-1}	[1]
$MnMoO_4$/CNF	Electrospinning	2.0 M KOH	389.7 F g^{-1} @ 0.1 A g^{-1}	92.1%, 5000 cycles @ 0.5 A g^{-1}	[2]
Rod-like α-$MnMoO_4$	Hydrothermal	2.0 M KOH	446.7 F g^{-1} @ 1 mA cm^{-2}	81.12%, 3000 cycles @ 8 mA cm^{-2}	[3]
α-$MnMoO_4$ nanorods	Hydrothermal	2.0 M KOH	551 F g^{-1} @ 1 A g^{-1}	89%, 1000 cycles @ 5 A g^{-1}	[4]
3D fan-like α-$MnMoO_4$	Precipitation	2.0 M KOH	562 F g^{-1} @ 1 A g^{-1}	99.8%, 1000 cycles @ 1 A g^{-1}	[5]
$MnMoO_4$/ $NiWO_4$	Hydrothermal	2.0 M KOH	598 F g^{-1} @ 1 A g^{-1}	82%, 5000 cycles @ 1 A g^{-1}	[6]
Co_3O_4/$MnMoO_4$	Hydrothermal	3.0 M KOH	663.75 F g^{-1} @ 2.5 mA cm^{-2}	95.32%, 3000 cycles @ 3 A g^{-1}	[7]
$NiCo_2O_4$/$MnMoO_4$	Hydrothermal	3.0 M KOH	1118 F g^{-1} @ 1 A g^{-1}	87.85%, 5000 cycles @ 1 A g^{-1}	[8]
$NiCo_2O_4$/$MnMoO_4$	Hydrothermal	3.0 M KOH	1169 F g^{-1} @ 2.5 mA cm^{-2}	92.58%, 5000 cycles @ 30 mA cm^{-2}	[9]
$NiCo_2S_4$/$MnMoO_4$	Hydrothermal	3.0 M KOH	1186.44 F g^{-1} @ 1 A g^{-1}	90.1%, 5000 cycles @ 10 A g^{-1}	[10]
$MnMoO_4$	Microwave synthesis	3.0 M KOH	1549 C g^{-1} @ 2 A g^{-1}	139%, 5000 cycles @ 5 A g^{-1}	[11]
MMO	Hydrothermal	3.0 M KOH	535.02 F g^{-1} @ 1 A g^{-1}	76.9%, 10000 cycles @ 5 A g^{-1}	**This work**
MMO-P	Hydrothermal	3.0 M KOH	701.22 F g^{-1} @ 1 A g^{-1}	87.4%, 10000 cycles @ 5 A g^{-1}	**This work**
MMO-C	Hydrothermal	3.0 M KOH	919.66 F g^{-1} @ 1 A g^{-1}	94.1%, 10000 cycles @ 5 A g^{-1}	**This work**

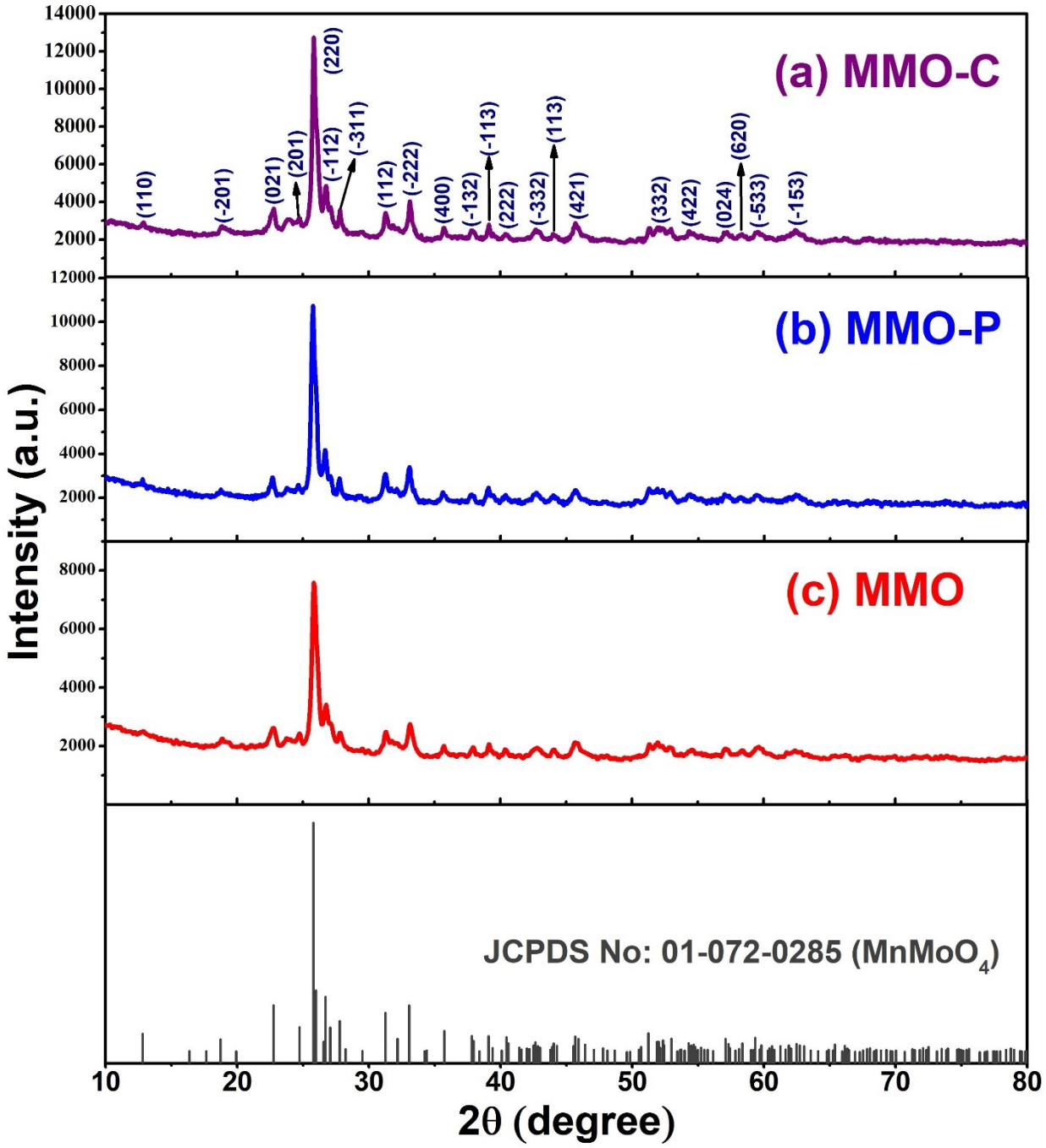

Fig. S1. XRD pattern of (a) MMO-C, (b) MMO-P and (c) MMO samples in comparison with their standard JCPDS data.

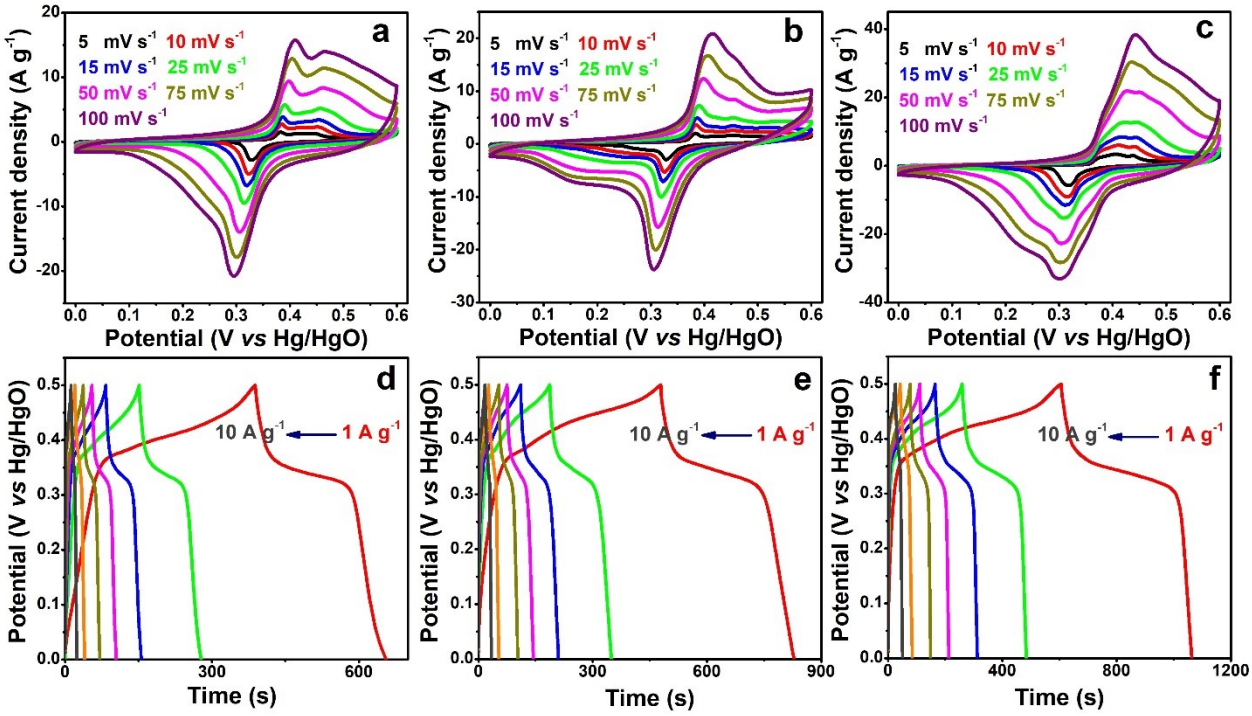

Fig. S2. CV curves (a, b, c) at different scan rates and GCD curves (d, e, f) at different current densities of MMO, MMO-P and MMO-C electrodes, respectively

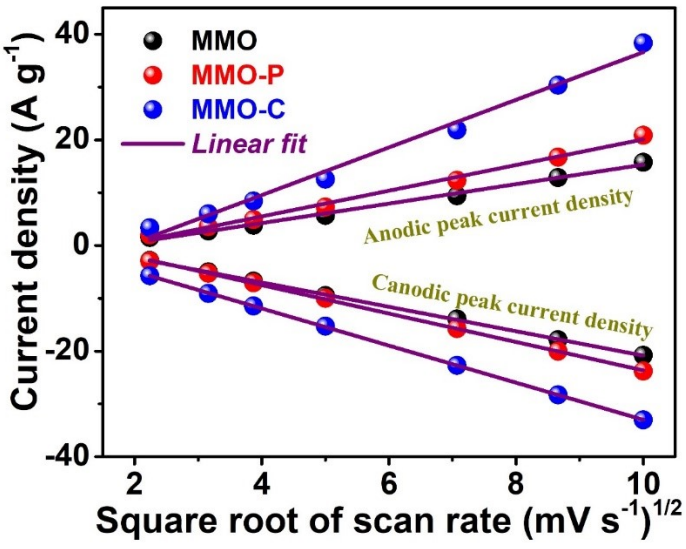

Fig. S3. Peak current density vs square root of scan rate plot of the MMO samples.

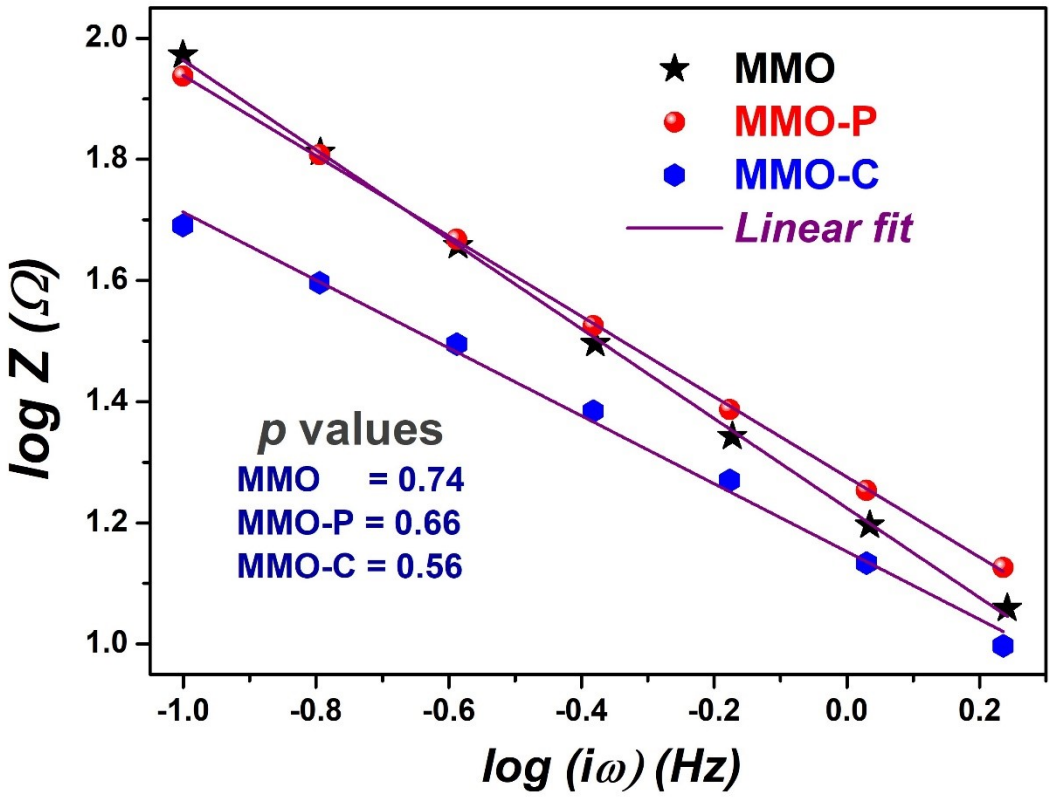

Fig S4. log Z vs log $(i\omega)$ plot of MMO samples with the determined *p*-values.

References

[1] Ghosh, D.; Giri, S.; Moniruzzaman, M.; Basu, T.; Mandal, M.; Das, C. K.; α-$MnMoO_4$/ Graphene Hybrid Composite: High Energy Density Supercapacitor Electrode Material. *Dalton Trans.* 2014, 43, 11067.

[2] Ahmad, M. W.; Anand, S.; Shalini, K.; Ul-Islam, M.; Yang, D. J.; Choudhury, C. $MnMoO_4$ Nanorods-Encapsulated Carbon Nanofibers Hybrid Mat as Binder-free Electrode for Flexible Asymmetric Supercapacitors. *Mater. Sci. Semicond. Process.* 2021, 136, 106176.

[3] Zhang, Y.; Teng, Y.; Li, Y.; Du, X.; Liu, L.; Wu, Y.; Meng, Y.; Hua, Y.; Zhao, X.; Liu, X. Microwave-assisted Green Synthesis of Manganese Molybdate Nanorods for High-Performance Supercapacitor. *Ionics* 2019, 25, 4361-4370.

[4] Jayasubramaniyan, S.; Balasundari, S.; Rayjada, P. A.; Satyanarayana, N.; Muralidharan, P. Microwave hydrothermal synthesis of α-$MnMoO_4$ nanorods for high electrochemical performance supercapacitors, *RSC Adv*., 2018, 8, 22559–22568.

[5] Wang, L. Q.; Yue, L. F.; Zang, X.; Zhu, H. Z.; Hao, X. P.; Leng, Z.; Liu, X. L. Chen, S. G. Synthesis of 3D α-$MnMoO_4$ Hierarchical Architectures for High-Performance Supercapacitor Applications, *CrystEngComm*, 2013, 18, 9286–9291.

[6] Feng, X. S.; Huang, Y.; Chen, M. H.; Chen, X. F.; Li, C.; Zhou, S. H.; Gao, X. G. Self-assembly of 3D hierarchical $MnMoO_4/NiWO_4$ microspheres for high-performance supercapacitor, *J. Alloys Compd.*, 2018, 763, 801–807.

[7] Cui, D. F.; Li, Y. F.; Li, Y. K.; Fan, Y. Y.; Chen, H. M.; Xu, H. Y.; Xue, C. Y. $Co_3O_4@MnMoO_4$ Nanorod Clusters as an Electrode Material for Superior Supercapacitors, *Int. J. Electrochem. Sci*., 2020, 15, 2776–2791.

[8] Gu, Z. X.; Zhang, X. J. $NiCo_2O_4@MnMoO_4$ Core-shell Flower for High-Performance Supercapacitors, *J. Mater. Chem. A*, 2016, 4, 8249–8254.

[9] Yuan, Y. L.; Wang, W. C.; Yang, J.; Tang, H. C.; Ye, Z. Z.; Zeng, Y. J.; Lu, J. G. Three-dimensional $NiCo_2O_4@MnMoO_4$ core-shell nanoarrays for high-performance asymmetric supercapacitors, *Langmuir*, 2017, 33, 10446–10454.

[10] Wei, X. J.; Li, Y. H.; Peng, H. R.; Liu, C. L.; Zhang, Y. H.; Xiao, P. Core-shell $NiCo_2S_4@MnMoO_4$ as an Advanced Electrode Material for High-performance Electrochemical Energy Storage, *ChemElectroChem*, 2017, 4, 2634–2642.

[11] Jabeen, S.; Kumar, P.; Samra, K. S. Boosting the electrochemical characteristics of $MnMoO_4$ nanoparticles for supercapacitor applications. *J. Appl. Electrochem*. 2023. https://doi.org/10.1007/s10800-023-02034-3.